Efficient and Stable Immobilization of TiO_2-Based Composite Photocatalytic System for Separation and Purification of Organic Pollutants in Wastewater under Solar Light

Aditya Sharma[a,c], Minami Yano[a], Cheng Zhang[a], Jie Ming[a], Xiang Sun[a], Yunxin Zhu[a], Guangqi An[a], Naoki Kawazoe[b], Guoping Chen[b], Yingnan Yang [a]*

[a]Graduate School of Life and Environmental Science, University of Tsukuba, 1-1-1 Tennodai, Tsukuba, Ibaraki 305-8571, Japan

[b]Research Center for Functional Materials, National Institute for Materials Sciences, 1-1-1 Namiki, Tsukuba, Ibaraki 305-0004, Japan

[c]Interdisciplinary Center for Catalytic Chemistry, Namiki, Tsukuba, Ibaraki 305-0004, Japan

*Corresponding Author. Tel/Fax: +81 29 8534650

E-mail address: yo.innan.fu@u.tsukuba.ac.jp (Y.Yang)

Abstract

Photocatalytic removal of organic pollutants emerging from untreated industrial and aquaculture wastewater are still limited by catalytic efficiency and stability in practical application. In this study, we have reported the development of silicone immobilized, hydrothermal and PEG assisted Ag doped TiO_2 composite (S-H-PEG/PAgT) system for an effective and sustainable elimination of organic pollutants under solar light illumination. Firstly, the newly developed silicone immobilized TiO_2 (S-TiO_2) was identified as an ideal strategy. It exhibited higher and stable organic pollutant removal (Rh B) than conventional immobilization methods, including poly-vinyl alcohol TiO_2 (PVA/TiO_2) and dip-coated TiO_2. Furthermore, the developed solar light driven S-H-PEG/PAgT photocatalytic system showed good light absorption, narrow band gap, crystalline phase, surface hydrophobicity, roughness, and excellent catalytic performance than S-TiO_2 (control). The S-H-PEG/PAgT was effective in removal of tetracycline (a model emerging organic contaminant) and exhibited high stability in a continuous (10 cycles) operation, meanwhile achieved good efficiency under different environmental conditions. The mechanism analysis revealed $^{\bullet}O_2^-$ and h^+ as dominant active species involved in the catalytic reaction. Most importantly, a synergistic effect of surface hydrophobicity, roughness and photocatalytic activity contributed to the overall reduction of pollutants. Therefore, the developed novel solar light driven S-H-PEG/PAgT photocatalytic system shows great promise for practical purification of organics pollutants in wastewater.

Keywords: Strategy of photocatalytic immobilization process, Efficiency of wastewater treatment, Elimination of antibiotics, Practical feasibility

1. Introduction

Water is the most vital component and valuable resource humans depend on for survival and development. In recent years, due to rapid industrialization and urbanization, water sources have been continuously polluted with emerging organic pollutants and antibiotics such as tetracycline (TC) [1,2]. The discharge of untreated, recalcitrant, toxic and non-degradable organic compounds poses a significant threat to the environment [3,4]. The unjustified use of antibiotics in aquaculture and other industries, as well as untreated wastewater with high concentrations of antibiotics contribute to the development of antibiotic resistant microorganisms that are harmful to human health, aquatic life, and biodiversity. Hence, wastewater treatment is critical for protecting water resources and advancing sustainable development. Therefore, a sustainable and efficient treatment is necessary for complete removal of emerging organic pollutants in wastewater.

Photocatalytic technology that utilizes solar as sustainable source of light has become a desirable green solution for treating environmental pollutants. The photocatalysts, including metal oxide semiconductors such as titanium dioxide (TiO_2), zinc oxide (ZnO), and tungsten dioxide (WO_3) have shown great potential for water treatment under UV irradiation. Among them, TiO_2 has gained much attention due to its superior activity, oxidizing ability, economic feasibility, and non-toxicity [5]. However, the recovery and reuse of TiO_2 nanoparticles in a slurry system is a fundamental problem, as it is time consuming, poor recoverability and practically difficult [6]. Stabilization of photocatalysts on solid supports can be an ideal option to increase the efficiency and reduce the operational costs in photocatalytic wastewater treatment [7].

In order to improve the feasibility of photocatalysts for practical application, the immobilization strategy should be economical, strongly fix photocatalysts on the surface of the support and have excellent photocatalytic activity. This reduces the loss of photocatalysts and improve the stability for a long term

use [8]. To achieve the above, several studies have been focused on identifying optimal stabilization technique and improving photocatalytic activity. Traditionally, the photocatalysts are immobilized on the supports by various approaches such as sol-gel technique, chemical vapor deposition (CVD), pulsed laser deposition (PVD), and solvent deposition [9]. The sol-gel method is used to immobilize photocatalysts by dip-coating supports in photocatalyst solution [10]. This method offers good controllability, dependability, and reproducibility in obtaining structured thin films [11]. But with dip-coated TiO_2 photocatalysts, it has been noted that formation of amorphous phase frequently resulted in low activity and poor charge separation [12]. To control the crystallinity, temperature and other reaction conditions needs to be monitored to achieve higher activity and stability in pollutant removal. The use polymer such as poly-vinyl alcohol (PVA) mixed with TiO_2 synthesized by sol-gel method are casted on supports under mild thermal treatment [13,14]. The thermal fixation of PVA/TiO_2 showed good activity and stability for 5 consecutive cycles. In another aspect, the use of polymeric binder such as polysiloxane is considered to be more convenient as it strongly fixes photocatalysts under ambient conditions and maintain good crystallinity and activity of TiO_2. Specifically, poly-siloxane binders seem to be a suitable option given their thermal stability, surface hydrophobicity, optical transparency, non-toxicity, and UV resistance. The TiO_2 photocatalyst uniformly combined with an oxime-based silicone binder in a continuous flow packed-bed reactor under UV light increased the photoactivity and durability [15]. Similarly, loading of photocatalysts on the siloxane increased activity and stability in consecutive cycles for organic reduction [16]. While silicone is optically transparent, mixing nanoparticles with the binder lowers the interaction of organics with the photocatalysts. A higher catalyst loading can overcome this problem, but, not feasible from the economical point of view. To date, the studies related to silicone binders are used after homogenization and there is also a lack of comparative studies with conventional immobilization methods. So, fixing the photocatalysts on silicone support could enhance the stability and durability, and their

activity in the continuous reactor should be compared with the existing immobilization methods. Additionally, the selection of support materials for fixing photocatalysts have an important function for ensuring process stability, catalytic performance, and development of immobilization system [17]. So, the glass beads coated with photocatalysts can be incorporated in multiple photocatalytic system and increase the interaction with the pollutants to achieve higher activity [18,19]. In addition, the solution parameters in an actual environmental also change depending on the pollution source [20]. However, little is known about the process stability and activity of photocatalytic surfaces for the removal of organic contaminants.

Besides, pure TiO_2 photocatalysts are only activated under UV light, which accounts for less than 5% of solar light. The rapid electron-hole recombination, low charge separation and wide band gap limits its scalability. Doping TiO_2 with noble metals (Ag, Au and Pt), non-metals (P, C, N and S) and narrow band semiconductors (Ag_2O and Ag_3PO_4) are known to effectively decrease original band gap and enhance photo-induced charge separation [21,22]. In our previous study, the doping of metal (Ag), metal oxides (Ag_2O and Ag_3PO_4) and non-metal (P) with TiO_2, synthesized by one-pot sol-gel/hydrothermal method showed superior performance in water splitting and organic dye degradation [23]. The quaternary heterostructure, hydrothermal synthesized Ag species doped TiO_2 based photocatalyst (H-PAgT) showed higher charge separation, small crystalline size, low electron-hole pair recombination than pure TiO_2. The H-PAgT photocatalyst immobilized on poly-siloxane showed strong adhesion of photocatalysts nanoparticles with good disinfection and pollutant removal efficiency [24,25]. In addition, several reports emphasize on the use of morphological tuners polyethylene glycol (PEG) during the synthesis process to further control grain growth and improve photocatalytic activity [26]. Until now, the effect of surface modifiers on H-PAgT immobilized system for removal of antibiotics has not yet been understood. Moreover, the underlying mechanism with different immobilization method is still unclear and requires further clarification. From practical perspective, a comprehensive assessment of catalytic performance and

stability needs to be evaluated to be adopted commercially. To the best of our knowledge, there is no study on H-PEG/PAgT immobilized system for treatment of wastewater.

Therefore, the main objective of this study was to identify the ideal immobilization strategy and develop a silicone immobilized, hydrothermal and PEG assisted Ag species TiO_2 based photocatalytic system (S-H-PEG/PAgT) for treatment of organic pollutants under solar light. We observed the reduction of organics with silicone immobilized TiO_2 (S-TiO_2) and S-H-PEG/PAgT photocatalysts. In the comparative study, the newly developed system showed better physio-chemical characteristics and stability compared to conventional dip-coated-TiO_2 and PVA/TiO_2 systems. Finally, the practical feasibility of the immobilized system for removal of organics was determined and the mechanism of the reaction was proposed.

2. Materials and methods

2.1 Preparation of hydrothermal synthesized Ag species doped TiO_2 based photocatalyst

The Ag species doped TiO_2 based photocatalysts was synthesized by hydrothermal method according to our previous study [23]. 6 mL of tetra-butyl titanate (TNBT) was added to 46 mL of ethanol was mixed thoroughly for 1 h (Solution A). A known amount of precursor salts $AgNO_3$ and Ag_3PO_4 was added to 1 mol L^{-1} of nitric acid (HNO_3) and sonicated until the salts were completely dissolved (Solution B). The solution B containing Ag and phosphate precursor mixture was added dropwise to solution A and stirred for 16 h to obtain a homogeneous and clear sol-gel at room temperature. The sol-gel solution was transferred to a hydrothermal reactor and treated at 120ºC for 3 h. After the reaction, the supernatant was washed 3 times with ethanol and distilled water. The supernatant was centrifuged three times at 5000 rpm and dried at 60ºC for 12 h to obtain H/PAgT. For the PEG-modified samples, PEG (1 g: 300 MW) and TNBT (6 mL) was added to 46 mL of ethanol and stirred for 1 hour (Solution A). The remaining steps are the same as those described previously. The sample that was obtained was denoted as H-PEG/PAgT.

2.2 Immobilization of TiO_2, H/PAgT and H-PEG/PAgT photocatalysts on silicone beads

The immobilization of photocatalysts on poly-siloxane binder was prepared according to our previous study [24], The glass beads were first washed with ethanol and distilled water and dried at 100ºC for 6 h. A commercially available poly-siloxane binder was coated on glass beads to cover the entire surface. 0.2 g of photocatalyst powders was loaded with the help of lab-designed sieve tube until the silicone supported glass surface was completely coated. The silicone supported beads were blow dried to remove any non-adherent nanoparticles and stored at room temperature for 24 h. After the curing process, the beads were washed with distill water to remove loosely attached nanoparticles on the surface and dried at room temperature. The amount of photocatalysts adhered on the surface on the beads were estimated to be around 0.023 mg. Silicone supported beads for TiO_2, PAgT and H-PEG/PAgT were denoted as S-TiO_2, S-H/PAgT and S-H-PEG/PAgT (S: silicone, PEG: polyethylene glycol, H: hydrothermal two step method, PAgT: P/Ag/Ag_2O/Ag_3PO_4/TiO_2 photocatalyst, and TiO_2: commercial P25), respectively. The glass beads coated with only silicone were used as a control.

2.3 Synthesis of dip-coated TiO_2 and PVA-TiO_2 coated beads

A sol-gel approach was followed for dip-coating TiO_2 on glass beads. Firstly, the glass beads were washed with methanol/water (30/70% w/w) and dried at 60ºC for 3 h. 1 g of P25 (TiO_2 Evonik Degussa) was added to methanol/water mixture (30/70% w/w) and sonicated for 15 min. 10 mL of dilute nitric acid (pH 3) was added slowly to above solution and stirred for 1 h. After 1 h of homogenization, glass beads were added to the TiO_2 dispersion and dried for 12 h at room temperature. The samples were calcined at 500ºC for 2 h. After calcination, the obtained dip coated samples were denoted as dip-coated TiO_2.

The PVA/TiO_2 coating was synthesized by adding 1 g of PVA and 0.5 g of TiO_2 to 20 mL of distilled water. The solution was stirred at 70ºC for 3 h with thermal magnetic stirrer. The PVA/TiO_2 was

115 coated by immersing glass beads in the solution. The coated glass beads were dried at 180ºC for 2 h to
116 obtain PVA/TiO_2 beads.

117 **2.4 Photocatalytic activity evaluation**

118 The catalytic activity of immobilized photocatalysts were evaluated by reduction of rhodamine B
119 (RhB) (model organic pollutant) and tetracycline (TC) (emerging organic pollutant) in a laboratory-
120 designed single-column reactor. The immobilized photocatalytic beads (0.14±0.02 g) thus synthesized
121 were packed in glass tubes (10cm, diameter: 1cm), which were connected with each other using plastic
122 connectors. One end of the connector was placed in a beaker containing Rh B (2 mg L^{-1}) /TC solution (10
123 mg L^{-1}) (50 mL). The connector was passed through a pump with a constant flow rate of 150 mL min^{-1},
124 facilitating the suction of pollutants from one end and through the fixed-bed photocatalytic reactor,
125 forming a cyclic system. The experiments were performed under simulated sunlight (550 W m^{-2}, XC-100,
126 SERIC ltd, USA) and 4 mL samples were taken at constant intervals. The experiments were all carried
127 out at ambient temperature and pH. For the comparative studies, the silicone immobilized TiO_2 beads was
128 replaced with dip-coated and PVA/TiO_2 coated beads. To effectively compare the catalyst activity, the
129 dosage of photocatalysts was kept constant at 0.16 g and experiment was conducted under the same
130 reaction condition as described above.

131 **3. Results and discussion**

132 **3.1 Characterization and identification of the optimal photocatalytic immobilization process**

133 The process of photocatalytic immobilization on glass beads by dip-coating, PVA and silicone are
134 described in section 2.3. Commercially available TiO_2 (P25) was employed as a model photocatalyst to
135 effectively compare and identify the optimal immobilization process. The immobilized photocatalysts was
136 firstly characterized, and activity of S-TiO_2 was compared with dip-coated TiO_2 and PVA/TiO_2
137 photocatalysts. The SEM measurements were conducted to understand the morphology of the S-TiO_2, dip-

coated TiO_2, and PVA/TiO_2 photocatalysts (Fig. 1a-c). In the dip-coated TiO_2, after calcination, two distinct catalysts layers stacked on each other were observed. The irregularity observed on dip-coated TiO_2 could be to due loss of poorly attached TiO_2 nanoparticles after washing (Fig.1a). Previous reports have also indicated the poor fixation of nanoparticles on glass surface by dip coating [27]. While in PVA/TiO_2, the crevasses are a result of thermal casting of TiO_2 photocatalysts with PVA (Fig.1b), which exhibit rough and porous structure. However, the homogenization of TiO_2 with PVA could hinder the interaction of pollutants with the active sites. On the other hand, the S-TiO_2 clearly displayed a rough surface with TiO_2 photocatalysts firmly attached on the silicone surface (Fig.1c). The silicone coated glass beads (control; No photocatalysts) showed smooth surface, typical for poly-siloxane materials (Fig. S1a-c). The addition of TiO_2 photocatalysts on silicone coated beads increased the surface roughness which could improve the light absorption and reaction sites with the pollutants [28]. Therefore, the S-TiO_2 could be beneficial for organic removal than dip-coated TiO_2 and PVA/TiO_2 photocatalysts.

To further investigate the surface texture and morphology, atomic force microscopy (AFM) measurement was carried out for the TiO_2 photocatalysts immobilized by different methods. As shown in Fig. 1d-i, the S-TiO_2 photocatalysts showed the highest surface roughness followed by PVA/TiO_2 and dip-coated TiO_2 photocatalysts. The average surface roughness observed in dip-coated TiO_2, PVA/TiO_2 and S-TiO_2, were 40.4, 69.3 and 74.9 nm, respectively. The surface roughness is consistent with the SEM images. The increase in surface roughness could improve the photocatalytic interaction with the pollutants and enhance the catalytic activity [29,30]. In addition, the surface roughness could improve the adsorption of pollutants, which would lead to higher catalytic activity upon irradiation. The higher surface roughness observed in S-TiO_2 and PVA/TiO_2 may improve overall catalytic adsorption and degradation of organic pollutants.

The surface wetting property of the immobilized photocatalysts involves the interaction of pollutants with the photocatalysts. The wettability of the surface is also governed by surface texture and roughness, in addition to their chemical property. The angle formed between the solid surface and the tangent drawn at the liquid drop was used to determine the wettability of the photocatalysts. As seen in Fig. 2, S-TiO_2 photocatalysts showed hydrophobic property with a contact angle of 121.4º, as compared to dip coated TiO_2 (5.3º) and PVA/TiO_2 (62.4º) photocatalysts. The pristine TiO_2 (0º) and silicone coated beads (92.3º) showed hydrophilic and hydrophobic property, respectively (Figure S1d-e). Usually, in the hydrophobic surface, a solid-liquid-air interface is formed which could be beneficial for interaction of pollutants with photocatalysts, and the oxidative species generated during the reaction process [31,32]. The increase in interaction and reaction with reactive species could drive the photocatalytic process and effectively reduce pollutants in wastewater. So, compared to hydrophilic surface, the hydrophobic surface could improve the photocatalytic activity of TiO_2 immobilized catalysts for pollutant removal in wastewater. Therefore, the increased surface roughness, and hydrophobicity of the S-TiO_2 immobilized photocatalysts may be beneficial for improving the activity and stability for wastewater treatment.

The photocatalytic activity of the immobilized TiO_2 photocatalysts was determined by the degradation of model organic pollutant Rh B. The experiments were conducted in a single packed column reactor and the initial dosage of photocatalysts from various immobilization methods were kept constant at 0.16 g/tube. Fig. 3a shows the catalytic performance of immobilized TiO_2 photocatalytic reduction of Rh B. As seen in the figure, the S-TiO_2 showed higher photocatalytic activity than dip-coated TiO_2 and PVA/TiO_2 photocatalysts. Rh B removal efficiency for PVA/TiO_2, dip-coated TiO_2, and S-TiO_2 photocatalysts were 43.7, 57.4, and 96.5%, respectively. The photocatalytic degradation rate of S-TiO_2 was 3.0 and 2.5 times faster than that of PVA/TiO_2 and dip-coated TiO_2 photocatalysts, respectively (Fig. S2). The increase in degradation rate can be attributed to the hydrophobic property of the S-TiO_2

183 immobilized photocatalyst. The hydrophobicity and surface roughness increased the interaction of the
184 pollutant with the photocatalysts at the solid-liquid interface [33,34]. The generated oxidative species at
185 the solid-liquid interface reduce organic pollutants resulting in higher photocatalytic efficiency. In the case
186 of PVA/TiO_2, the homogenization of TiO_2 in the PVA matrix could restricts the interaction of
187 photocatalysts with the pollutants and block the active site, leading to low activity. Similarly, the dip-
188 coated TiO_2 photocatalyst could form amorphous TiO_2, which generally exhibits poor activity. These
189 results demonstrated the superior catalytic performance of S-TiO_2 immobilized photocatalytic system than
190 PVA/TiO_2 and dip-coated TiO_2 photocatalysts.

191 In practical application, the stability of the photocatalysts determines its economic feasibility and
192 catalytic performance. A 10-cycle repetitive experiments were conducted to investigate the stability of S-
193 TiO_2, PVA/TiO_2 and dip-coated TiO_2 photocatalysts. As seen Fig. 3b, the S-TiO_2 photocatalysts showed
194 the highest degradation efficiency than PVA/TiO_2 and dip-coated TiO_2 photocatalysts after 30 min of
195 irradiation. The Rh B degradation efficiency of S-TiO_2 were constant throughout the 10-cycle and reached
196 a degradation efficiency of 96.5% (10^{th} cycle). The degradation efficiency of PVA/TiO_2 and dip-coated
197 TiO_2 after 10 cycles were 49.7% and 52.3%, respectively. For dip-coated TiO_2 and PVA/TiO_2, a slight
198 decrease in activity and relatively unstable performance was observed, mainly due to the loss of poorly
199 attached photocatalysts on the glass beads. This was confirmed by SEM images observed before and after
200 10 cycles. In comparison with the SEM of before samples (Fig. 1a-b), a significant loss of photocatalysts
201 could be seen in dip-coated TiO_2 and PVA/TiO_2 after reaction (Fig. 3c-d). On the other hand, the
202 morphology of S-TiO_2 remains unchanged even after 10 cycles, and no photocatalytic loss was observed
203 (Fig. 3e). This suggests that S-TiO_2 immobilized strategy strongly fixed the photocatalysts on the support
204 material, which led to improved photocatalytic activity for removal of pollutants. Therefore, the
205 immobilization of TiO_2 nanoparticles on silicone was found to be an ideal strategy for improving the

206 photocatalytic activity, stability, and reliability than conventional methods for treating organic pollutants
207 in wastewater.

208 **3.2 Development of solar light driven S-H-PEG/PAgT photocatalytic system for TC removal**

209 In the photocatalytic system, the use of pristine TiO_2 (P25) is limited only to UV light, which
210 accounts for less than 5% of the solar light and restricts the potential use of visible light (> 40% solar
211 light). To address this issue, S-H-PEG/PAgT photocatalytic system was developed and used in future
212 experiments using TC as a representative model organic pollutant in wastewater under solar light. The S-
213 H-PEG/PAgT photocatalysts was characterized by SEM, AFM, WCA, UV-vis and XRD. The morphology
214 of S-H/PAgT (control) and S-H-PEG/PAgT are shown in Fig. S3a-b. As seen in the figure, the S-H/PAgT
215 and S-H-PEG/PAgT showed irregular morphology, as compared to S-TiO_2 photocatalysts (Fig. 1c). It has
216 been noted that PEG could effectively control the morphology and crystalline size of TiO_2 modified
217 photocatalysts [35]. The PEG addition during hydrothermal synthesis could control the grain growth, and
218 lead to small particle size [36]. The small particle size and irregular structure of S-H-PEG/PAgT could
219 significantly increase surface roughness and improves the pollutant adsorption, and higher catalytic
220 activity. The surface texture of the photocatalysts was determined by the AFM measurement. As illustrated
221 in Fig. S3c-f, the S-H/PAgT and S-H-PEG/PAgT photocatalysts exhibited the highest surface roughness
222 than S-TiO_2 (Fig. 1f and i). The higher average peak to valley value (Ra=2349 nm) observed in the S-
223 H/PAgT photocatalysts could be due to the large particle size attached on the surface of silicone coated
224 beads. In S-H-PEG/PAgT photocatalysts, the addition of PEG surfactant during the synthesis process
225 controlled the grain growth resulting in smaller NPs fixed on silicone coated beads and lower peak to
226 valley (Ra=1698 nm). The observations are in accordance with the SEM images (Fig. S3a-b). The surface
227 light absorption and scattering characteristics depend on roughness around the wavelength of the incident

light. For the above reasons, increased surface roughness in S-H/PAgT and S-H-PEG/PAgT could further improve light absorption and lead to improved activity in wastewater treatment.

Fig. S3g-h shows the surface wetting property of the silicone immobilized TiO_2 based composite photocatalysts. The water contact angle of S-H-PEG/PAgT and S-H/PAgT photocatalysts were 134.2º and 125.7º, respectively. As mentioned before, the silicone (control) surface is hydrophobic in nature. The S-H-PEG/PAgT photocatalysts showed ultra-hydrophobic surface due to the irregular morphology, and small particle size. The addition of PEG during the synthesis process could have influenced the surface texture and hydrophobicity. The ultra-hydrophobic surface could improve the adsorption and interaction of pollutants. The improved interaction on the surface also increases adsorption of surface oxygen to generate super oxide anions, leading to higher photocatalytic activity. Hence, the ultra-hydrophobic surface of S-H-PEG/PAgT may improve activity and stability for long-term practical elimination under solar light irradiation.

The light absorption ability of TiO_2 and TiO_2 based composite photocatalysts immobilized on silicone are shown in Fig. 4a. The S-H-PEG/PAgT photocatalysts showed the highest light absorption both in the UV and visible light range compared to S-H/PAgT and S-TiO_2 photocatalysts. The strong absorption absorbed in the visible light region (400-800 nm) could be due to the surface plasmon resonance (SPR) effect coming from light responsive Ag salts [37], which is present in both S-H-PEG/PAgT and S-H/PAgT photocatalysts. The addition of Ag salts improves the light absorption, and significant red shift into the visible light region, according to the previous reports [22]. Additionally, the better optical property in S-H-PEG/PAgT can be owed to the addition of surfactants (PEG), which reduces grain growth and further improves light absorption. Moreover, the surface texture and roughness in S-H-PEG/PAgT could improve light scattering and absorption (Table S1). The calculated band gap of S-H-PEG/PAgT, S-H/PAgT and S-TiO_2 photocatalysts were 2.98, 3.10 and 3.17 eV. The narrow band gap, and

improved light absorption ability of S-H-PEG/PAgT could effectively increase the generation of reactive species, and charge separation for reduction of pollutants under solar light irradiation.

Fig. 4b shows the XRD patterns of S-TiO_2 and TiO_2 based composite photocatalysts. As shown in figure, the crystalline phase of S-H-PEG/PAgT and S-H/PAgT showed the presence of only anatase phase of TiO_2. While S-TiO_2 showed both anatase and rutile phase of TiO_2, typical observation for P25 photocatalysts [38]. The Anatase phase of TiO_2 is considered to be more active under visible light irradiation and could result in higher catalytic performance for wastewater treatment [39]. The slightly better crystallinity observed in S-H-PEG/PAgT photocatalyst are a result of the addition of PEG. The addition of surfactant during the synthesis process control the grain growth and effectively improve its crystallinity [40]. In addition, the S-H-PEG/PAgT and S-H/PAgT showed the presence of Ag salts (Ag_2O/Ag_3PO_4) [24]. The presence of Ag salts in the XRD patterns confirms the increased light absorption resulted from the SPR effect observed in both S-H-PEG/PAgT and S-H/PAgT (Fig. 4a). The superior characteristics of S-H-PEG/PAgT photocatalysts with higher surface roughness, hydrophobicity, narrow band gap, good optical property, and better crystallinity could improve photocatalytic activity in removal of pollutants from wastewater under solar light irradiation.

The photocatalytic activity of the silicone immobilized S-H-PEG/PAgT was evaluated by degradation of model emerging organic pollutant tetracycline (TC). As seen in Fig. 4c, higher TC removal was observed with S-H-PEG/PAgT photocatalyst compared to S-H/PAgT, and S-TiO_2. The poor removal of TC in silicone (control) suggested that the removal occurred through the photocatalytic generation of oxidative species rather than adsorption. The rate of TC degradation efficiency for S-H-PEG/PAgT, S-H/PAgT, and S-TiO_2, was 0.0278, 0.0202 and 0.0106 min^{-1}, respectively (Fig. 4d). The irregular morphology and hydrophobicity in S-H-PEG/PAgT photocatalyst could contribute to increased interaction with pollutants, and generation of reactive species, which led to higher photocatalytic activity. In addition,

the S-H-PEG/PAgT showed higher TOC removal compared of other modified samples (Fig. S4). Furthermore, the S-H-PEG/PAgT photocatalysts showed high activity in comparison with the reported literatures (Table S2). Although, a direct comparison with the existing literature would be difficult considering the difference in various reaction parameters, but the S-H-PEG/PAgT photocatalysts showed better performance under ambient conditions. Thus, the above results clarify the S-H-PEG/PAgT photocatalyst with small particles size, average surface roughness, good light absorption and effective removal of organics from wastewater.

3.3 Practical feasibility of S-H-PEG/PAgT photocatalytic system

The photocatalytic activity in real environmental is affected by various factors such as flow rate, pH, light intensity, and temperature. Therefore, the efficiency of S-H-PEG/PAgT photocatalysts was investigated under various influencing factors to mimic the environmental conditions.

The flow rate in the photocatalytic reaction is one of the important parameters that affects the TC degradation efficiency. The effect of flow rates on TC removal is shown in Fig. 5a. The photocatalytic activity remained significantly higher in flow rates from 50 mL to 250 mL min^{-1}. The degradation efficiency at 50-, 150- and 250-mL min^{-1} were 85.1, 85.9 and 86.2%, respectively. The pseudo-first order kinetics of the reaction for 50-, 150- and 250-mL min^{-1} were 2.243 x 10^{-2}, 2.788 x 10^{-2}, and 2.560 x 10^{-2} min^{-1}, respectively. The flow rate determines the rate of mass transfer and catalytic interaction with the pollutants [6]. The high activity observed from low-high flow rate suggested effective mass transfer and activity. The high activity achieved under different flow rates illustrated that the S-H-PEG/PAgT photocatalysts could be used in various photocatalytic systems with varying flow rates to obtain effective reduction of pollutants.

The photocatalytic removal of organic materials is significantly influenced by the pH of the solution. The influence of initial pH on S-H-PEG/PAgT photocatalytic removal of TC was investigated

297 from pH 3 to 9. As shown in Fig. 5b, the degradation efficiency increased from pH 3 to 5, and plateaued
298 at pH 7 before significantly decreasing at pH 9. The TC degradation efficiency observed at pH 3, 5, 7 and
299 9 were 77.4, 96.7, 93.2 and 54.3%, respectively. The optimal pH was observed to be around pH 5 to 7.
300 The pH_{pzc} value of TiO_2 photocatalysts are around pH 6.8 [41], and the pKa value of TC pH 5.0 to 6.7.
301 The S-H-PEG/PAgT at pH 5 have a positive charge, which TC is in the zwitterion state. Hence, the
302 interaction between the TC and S-H-PEG/PAgT increases at pH 5 to 7, and led to higher photocatalytic
303 conversion [42]. On the other hand, the degradation is less favorable at acidic (pH 3) and alkaline (pH 9)
304 due to differences the surface property. This shows that the S-H-PEG/PAgT photocatalyst can effectively
305 reduce TC at pH 5 to 7 in environmental conditions.
306 Fig 5c shows dependence of photocatalytic activity on temperature from 10 to 50 °C. The TC
307 removal achieved at 10-20, 20-30, 30-40, and 40-50 °C were 76.3, 85.5, 86.3 and 86.4% respectively. As
308 observed in the figure, the rise in temperature from 10 to 20 °C increased the photocatalytic activity, and
309 remained consistent from 20 to 50 °C. The significant reduction observed at such low temperature (10 °C),
310 infers that the TC reduction is predominantly depended on light activation rather than temperature. These
311 findings are consistent with our previous studies conducted at low to high temperature [43]. The optimal
312 temperature for photocatalytic TC reduction was observed to be in the range of 20 to 50 °C and is efficient
313 under real temperature observed in the environment.
314 The dependence of TC degradation on incident light intensity was investigated in the range of 100
315 to 1000 W m^{-2}. As shown in Fig 5d, a slight increase in photocatalytic activity was observed with increase
316 in light intensity from 100 to 550 W m^{-2}, while TC reduction from 550 to 1000 W m^{-2} remained unchanged.
317 The TC degradation efficiency observed at 100, 300, 550, 700, and 1000 Wm^{-2} were 78.4, 79.5, 88.5, 89.1
318 and 89.4% respectively. The marginal difference in catalytic performance at low to high intensity is
319 attributed to the higher catalytic activity of the synthesized photocatalysts. This indicates that the even at

low light intensity, high charge separation can be achieved for the generation of reactive species resulting in higher TC reduction. The results suggest that the photocatalyst is effective in real environmental conditions from low to high light intensity for reduction of pollutants. The S-H-PEG/PAgT photocatalytic activity demonstrates the ability for effective remediation of organic contaminants under different influencing factors in real environmental (pH, temperature, light intensity) and reactor condition (flow rate) for practical application.

The feasibility and stability of S-H-PEG/PAgT photocatalytic system for practical application was investigated by repetitive experiments (10 cycles). As shown in Fig. 6a, the TC degradation efficiency from 1^{st} (94.6%) to 10^{th} (91.3%) cycle remained significantly higher demonstrating the superior S-H-PEG/PAgT catalytic performance in pollutant removal. The high surface roughness and irregular morphology of nanoparticles ensured good contact with the pollutants and improved catalytic removal in repetitive experiments. The XRD patterns showed the crystallinity and crystalline phase remained the same and strong peaks associated with TiO_2 (Anatase) was visible after 10 cycles (Fig. 6b). Similarly, SEM images showed no change in morphology and surface texture after the reaction (Fig. 6c-d). The hydrophobic surfaces have high stability and increase reusability of the photocatalyst materials [44]. In general, after prolonged exposure to organic pollutants, the surface is contaminated with unreacted organics which affect the surface wetting property or loss of nanoparticles reduce catalytic activity. In this study, the morphology and surface hydrophobicity were retained after reaction, further illustrating the durability of the photocatalytic materials (Fig. 6e-f). Therefore, the S-H-PEG/PAgT photocatalysts with high stability and activity shows promise for the treatment of organic pollutants in practical application.

3.4 Mechanism of S-H-PEG/PAgT photocatalysts for wastewater treatment

The purpose of the scavenger studies was to ascertain the contribution of reactive species to the photocatalytic reduction of TC by S-H-PEG/PAgT under solar light. As shown in Figure 7a, the addition

of 1-4BQ significantly suppressed the S-H-PEG/PAgT photocatalytic degradation of TC, indicating that $O_2^{\bullet-}$ as the predominant species involved in the degradation process. Moreover, the activity also reduced after the addition of EDTA, suggesting that h^+ was the main species involved in the reaction. On the other hand, the addition of •OH had no effect on TC removal and was not a direct contributor to the photocatalytic reaction. The predominant reactive species observed in this study are in accordance with our previous results with H/PAgT photocatalysts in the slurry system [23]. Therefore, $O_2^{\bullet-}$ and h^+ were found to be the key species driving S-H-PEG/PAgT photocatalytic pollutant removal in wastewater.

Figure 7b-c shows the proposed mechanism for S-H-PEG/PAgT composite photocatalysts for degradation of organic pollutants under solar light irradiation. Based on the aforementioned results and discussion, the S-H-PEG/PAgT showed superior photocatalytic activity and stability than conventional immobilization methods. The improved photocatalytic activity could be attributed to the following: The photocatalyst upon light irradiation, e^- and h^+ are generated at the CB and VB position. As the flow of e^- and h^+ in TiO_2, Ag_3PO_4, Ag_2O are governed by the fermi levels [45], the h^+ flows to the higher fermi level ($TiO_2 \rightarrow Ag_2O \rightarrow Ag_3PO_4$), while e^- move to the lower fermi level ($Ag_3PO_4 \rightarrow Ag_2O \rightarrow Ag$) (Fig. 7b). The e^- and h^+ on reaction with adsorbed water and surface oxygen, $O_2^{\bullet-}$ and h^+ are generated which effectively reduce pollutants (Fig. 7a); Subsequently, the increase in surface roughness due to irregular morphology of S-H-PEG/PAgT photocatalysts could enhance the interaction between the pollutants and photocatalysts (Fig. 7c). The addition of PEG effectively controls the grain growth, and particle size of the photocatalysts, which further increase the light absorption and activity under visible light irradiation (Fig. 4a-b). The improved interaction with the photocatalysts could effectively react with generated active species and reduce pollutants; the ultra-hydrophobic property (134.3°) of S-H-PEG/PAgT photocatalyst was found to improve the photocatalytic stability in long-term treatment of organics. Typically, a solid-liquid-air interface is formed in the hydrophobic surface, which may be advantageous for the interaction

of pollutants with photocatalysts and increased generation of surface oxidative species during the reaction process could affect positively on the reaction process. Thus, an interaction between photocatalytic activity, the irregular morphology**,** roughness, and ultra-hydrophobicity contributed to the overall activity and stability of S-H-PEG/PAgT photocatalysts. Therefore, the developed photocatalytic immobilized system shows great promise as a green alternative for efficient and durable treatment of organics pollutants in wastewater under solar light irradiation.

4. Conclusion

In this study, a silicone immobilized TiO_2 (S-TiO_2) was identified as an ideal strategy of photocatalytic immobilization. In addition, the silicone immobilized, hydrothermal and PEG assisted Ag species doped TiO_2 composite photocatalytic system was developed as an efficient and sustainable method for degradation of pollutants under solar light irradiation. The S-H-PEG/PAgT photocatalysts showed good light absorption, narrow band gap, better crystallinity, higher surface roughness, hydrophobicity, and improved catalytic performance than S-TiO_2 (control). Moreover, an effective removal of pollutants under different environmental factors and high stability in repetitive treatment demonstrates the feasibility in real application. Scavenger study revealed $^{\bullet}O_2^-$ and h^+ as the dominant reactive species contributed to the removal of TC. The S-H-PEG/PAgT photocatalyst surface hydrophobicity, surface roughness, and photocatalytic activity work in concert to remove organic contaminants from wastewater. Therefore, the solar light driven S-H-PEG/PAgT photocatalyst shows great potential in practical treatment of emerging organic pollutants in wastewater.

Acknowledgements

This work was supported by Scientific Research (B) 22H03778 and Grant-in-Aid for Exploratory Research 21k19628 from Japan Society for the Promotion of Science. The authors would like to thank

National Institute of Materials Science (NIMS) for their technical support with characterization of photocatalyst materials.

Author contributions

Aditya Sharma: Formal analysis, Investigation, Methodology, Writing-Original Draft and Editing. **Minami Yano:** Formal analysis, Investigation, Methodology, Validation. **Cheng Zhang:** Writing-Review and Editing**,** Investigation. **Jie Ming:** Investigation, Validation. **Xiang Sun:** Investigation, Validation. **Yunxin Zhu:** Writing-Review and Editing. **Guangqi An**: Writing-Review and Editing. **Naoki Kawazoe:** Resources, Methodology, Editing. **Guoping Chen:** Resources, Methodology, Writing-Review and Editing**. Yingnan Yang:** Conceptualization, Methodology, Validation, Funding acquisition, Resources, Project administration, Supervision, Writing-Review and Editing.

References

[1] N. Roy, S.A. Alex, N. Chandrasekaran, A. Mukherjee, K. Kannabiran, A comprehensive update on antibiotics as an emerging water pollutant and their removal using nano-structured photocatalysts, J. Environ. Chem. Eng. 9 (2021) 104796. https://doi.org/10.1016/j.jece.2020.104796.

[2] S. Khan, M. Naushad, M. Govarthanan, J. Iqbal, S.M. Alfadul, Emerging contaminants of high concern for the environment: Current trends and future research, Environ. Res. 207 (2022) 112609. https://doi.org/10.1016/j.envres.2021.112609.

[3] Y. Zhou, W. bing Li, V. Kumar, M.C. Necibi, Y.J. Mu, C. ze Shi, D. Chaurasia, S. Chauhan, P. Chaturvedi, M. Sillanpää, Z. Zhang, M.K. Awasthi, R. Sirohi, Synthetic organic antibiotics residues as emerging contaminants waste-to-resources processing for a circular economy in China: Challenges and perspective, Environ. Res. 211 (2022) 113075. https://doi.org/10.1016/j.envres.2022.113075.

[4] N. Morin-Crini, E. Lichtfouse, M. Fourmentin, A.R.L. Ribeiro, C. Noutsopoulos, F. Mapelli, É.

411 Fenyvesi, M.G.A. Vieira, L.A. Picos-Corrales, J.C. Moreno-Piraján, L. Giraldo, T. Sohajda, M.M.
412 Huq, J. Soltan, G. Torri, M. Magureanu, C. Bradu, G. Crini, Removal of emerging contaminants
413 from wastewater using advanced treatments. A review, Environ. Chem. Lett. 20 (2022) 1333–1375.
414 https://doi.org/10.1007/s10311-021-01379-5.
415 [5] D. Chen, Y. Cheng, N. Zhou, P. Chen, Y. Wang, K. Li, S. Huo, P. Cheng, P. Peng, R. Zhang, L.
416 Wang, H. Liu, Y. Liu, R. Ruan, Photocatalytic degradation of organic pollutants using TiO2-based
417 photocatalysts: A review, J. Clean. Prod. 268 (2020) 121725.
418 https://doi.org/10.1016/j.jclepro.2020.121725.
419 [6] R. Binjhade, R. Mondal, S. Mondal, Continuous photocatalytic reactor: Critical review on the
420 design and performance, J. Environ. Chem. Eng. 10 (2022) 107746.
421 https://doi.org/10.1016/j.jece.2022.107746.
422 [7] S. Mozia, Photocatalytic membrane reactors (PMRs) in water and wastewater treatment. A review,
423 Sep. Purif. Technol. 73 (2010) 71–91. https://doi.org/10.1016/J.SEPPUR.2010.03.021.
424 [8] C.S. Lugo-Vega, B. Serrano-Rosales, H. de Lasa, Immobilized particle coating for optimum photon
425 and TiO2 utilization in scaled air treatment photo reactors, Appl. Catal. B Environ. 198 (2016) 211–
426 223. https://doi.org/10.1016/j.apcatb.2016.05.063.
427 [9] K. Fouad, M. Bassyouni, M.G. Alalm, M.Y. Saleh, Recent developments in recalcitrant organic
428 pollutants degradation using immobilized photocatalysts, Appl. Phys. A Mater. Sci. Process. 127
429 (2021) 1–28. https://doi.org/10.1007/s00339-021-04724-1.
430 [10] M. Samy, M.G. Ibrahim, M. Gar Alalm, M. Fujii, Effective photocatalytic degradation of
431 sulfamethazine by CNTs/LaVO4 in suspension and dip coating modes, Sep. Purif. Technol. 235
432 (2020) 116138. https://doi.org/10.1016/J.SEPPUR.2019.116138.
433 [11] A.M. Nasir, J. Jaafar, F. Aziz, N. Yusof, W.N.W. Salleh, A.F. Ismail, M. Aziz, A review on floating

nanocomposite photocatalyst: Fabrication and applications for wastewater treatment, J. Water Process Eng. 36 (2020) 101300. https://doi.org/10.1016/j.jwpe.2020.101300.

[12] D. Wood, S. Shaw, T. Cawte, E. Shanen, B. Van Heyst, An overview of photocatalyst immobilization methods for air pollution remediation, Chem. Eng. J. 391 (2020) 123490. https://doi.org/10.1016/j.cej.2019.123490.

[13] S. Sakarkar, S. Muthukumaran, V. Jegatheesan, Evaluation of polyvinyl alcohol (PVA) loading in the PVA/titanium dioxide (TiO2) thin film coating on polyvinylidene fluoride (PVDF) membrane for the removal of textile dyes, Chemosphere. 257 (2020) 127144. https://doi.org/10.1016/J.CHEMOSPHERE.2020.127144.

[14] V. Soltaninejad, A. Maleki, A green, and eco-friendly bionanocomposite film (poly(vinyl alcohol)/TiO2/chitosan/chlorophyll) by photocatalytic ability, and antibacterial activity under visible-light irradiation, J. Photochem. Photobiol. A Chem. 404 (2021) 112906. https://doi.org/10.1016/J.JPHOTOCHEM.2020.112906.

[15] D.S. Kim, Y.S. Park, Photocatalytic decolorization of rhodamine B by immobilized TiO2 onto silicone sealant, Chem. Eng. J. 116 (2006) 133–137. https://doi.org/10.1016/j.cej.2005.10.013.

[16] M. Gar Alalm, M. Samy, S. Ookawara, T. Ohno, Immobilization of S-TiO2 on reusable aluminum plates by polysiloxane for photocatalytic degradation of 2,4-dichlorophenol in water, J. Water Process Eng. 26 (2018) 329–335. https://doi.org/10.1016/j.jwpe.2018.11.001.

[17] B. Srikanth, R. Goutham, R. Badri Narayan, A. Ramprasath, K.P. Gopinath, A.R. Sankaranarayanan, Recent advancements in supporting materials for immobilised photocatalytic applications in waste water treatment, J. Environ. Manage. 200 (2017) 60–78. https://doi.org/10.1016/j.jenvman.2017.05.063.

[18] C. Shen, Y.J. Wang, J.H. Xu, G.S. Luo, Facile synthesis and photocatalytic properties of TiO2

nanoparticles supported on porous glass beads, Chem. Eng. J. 209 (2012) 478–485. https://doi.org/10.1016/j.cej.2012.08.044.

[19] H. Khalilian, M. Behpour, V. Atouf, S.N. Hosseini, Immobilization of S, N-codoped TiO2 nanoparticles on glass beads for photocatalytic degradation of methyl orange by fixed bed photoreactor under visible and sunlight irradiation, Sol. Energy. 112 (2015) 239–245. https://doi.org/10.1016/j.solener.2014.12.007.

[20] N. Abd Rahman, C.E. Choong, S. Pichiah, I.W. Nah, J.R. Kim, S.E. Oh, Y. Yoon, E.H. Choi, M. Jang, Recent advances in the TiO2 based photoreactors for removing contaminants of emerging concern in water, Sep. Purif. Technol. 304 (2023) 122294. https://doi.org/10.1016/j.seppur.2022.122294.

[21] A. Kumar, P. Choudhary, A. Kumar, P.H.C. Camargo, V. Krishnan, Recent Advances in Plasmonic Photocatalysis Based on TiO2 and Noble Metal Nanoparticles for Energy Conversion, Environmental Remediation, and Organic Synthesis, Small. 18 (2022) 2101638. https://doi.org/10.1002/smll.202101638.

[22] D. Kanakaraju, F.D. anak Kutiang, Y.C. Lim, P.S. Goh, Recent progress of Ag/TiO2 photocatalyst for wastewater treatment: Doping, co-doping, and green materials functionalization, Appl. Mater. Today. 27 (2022) 101500. https://doi.org/10.1016/j.apmt.2022.101500.

[23] Q. Zhu, N. Liu, Q. Ma, A. Sharma, D. Nagai, X. Sun, C. Zhang, Y. Yang, Sol-gel/hydrothermal two-step synthesis strategy for promoting Ag species–modified TiO2-based composite activity toward H2 evolution under solar light, Mater. Today Energy. 20 (2021) 100648. https://doi.org/10.1016/j.mtener.2021.100648.

[24] A. Sharma, J. Ming, N. Liu, X. Sun, Y. Zhu, M. Yano, G. Chen, Y. Yang, Sustainable and efficient reduction of pollutants by immobilized PEG-P/Ag/Ag2O/Ag3PO4/TiO2 photocatalyst for

purification of saline wastewater, Mar. Pollut. Bull. 179 (2022) 113731. https://doi.org/10.1016/j.marpolbul.2022.113731.

[25] N. Liu, J. Ming, A. Sharma, X. Sun, N. Kawazoe, G. Chen, Y. Yang, Sustainable photocatalytic disinfection of four representative pathogenic bacteria isolated from real water environment by immobilized TiO2-based composite and its mechanism, Chem. Eng. J. 426 (2021) 131217. https://doi.org/10.1016/j.cej.2021.131217.

[26] A. Sengele, D. Robert, N. Keller, C. Colbeau-Justin, V. Keller, Sn-doped and porogen-modified TiO2 photocatalyst for solar light elimination of sulfure diethyle as a model for chemical warfare agent, Appl. Catal. B Environ. 245 (2019) 279–289. https://doi.org/10.1016/j.apcatb.2018.12.071.

[27] A. Bouarioua, M. Zerdaoui, Photocatalytic activities of TiO2 layers immobilized on glass substrates by dip-coating technique toward the decolorization of methyl orange as a model organic pollutant, J. Environ. Chem. Eng. 5 (2017) 1565–1574. https://doi.org/10.1016/j.jece.2017.02.025.

[28] S. Roberto Andrade Dantas, R.C. de Oliveira Romano, F. Vittorino, K. Loh, Effects of surface roughness and light scattering on the activation of TiO2 on mortar photocatalytic process, Constr. Build. Mater. 270 (2021) 121421. https://doi.org/10.1016/j.conbuildmat.2020.121421.

[29] Y. Zhang, E.K. Stefanakos, D. Yogi Goswami, Effect of photocatalytic surface roughness on reactors effectiveness for indoor air cleaning, Build. Environ. 61 (2013) 188–196. https://doi.org/10.1016/j.buildenv.2012.12.018.

[30] S. Teekateerawej, J. Nishino, Y. Nosaka, Design and evaluation of photocatalytic micro-channel reactors using TiO2-coated porous ceramics, J. Photochem. Photobiol. A Chem. 179 (2006) 263–268. https://doi.org/10.1016/j.jphotochem.2005.08.024.

[31] X. Sheng, Z. Liu, R. Zeng, L. Chen, X. Feng, L. Jiang, Enhanced Photocatalytic Reaction at Air-Liquid-Solid Joint Interfaces, J. Am. Chem. Soc. 139 (2017) 12402–12405.

https://doi.org/10.1021/jacs.7b07187.

[32] L. Zhang, L. Rao, P. Wang, Z. Shi, P. Wang, Superhydrophobic self-floating TiO2-silicone composite aerogels and their air–liquid-solid triphase photocatalytic system, Appl. Surf. Sci. 536 (2021) 147726. https://doi.org/10.1016/j.apsusc.2020.147726.

[33] J. Liu, L. Ye, S. Wooh, M. Kappl, W. Steffen, H.J. Butt, Optimizing Hydrophobicity and Photocatalytic Activity of PDMS-Coated Titanium Dioxide, ACS Appl. Mater. Interfaces. 11 (2019) 27422–27425. https://doi.org/10.1021/acsami.9b07490.

[34] Y. Zhang, Y. Chen, C. Wang, Z. Fan, Y. Wang, A multifunctional composite membrane with photocatalytic, self-cleaning, oil/water separation and antibacterial properties, Nanotechnology. 33 (2022) 355703. https://doi.org/10.1088/1361-6528/ac6ff4.

[35] X. Hu, Q. Zhu, Z. Gu, N. Zhang, N. Liu, M.S. Stanislaus, D. Li, Y. Yang, Wastewater treatment by sonophotocatalysis using PEG modified TiO2 film in a circular Photocatalytic-Ultrasonic system, Ultrason. Sonochem. 36 (2017) 301–308. https://doi.org/10.1016/j.ultsonch.2016.12.008.

[36] P. Balaganapathi, T.; Kaniamuthan, B.; Vinoth, S.; Thailakan, PEG assisted synthesis of porous TiO2 using sol-gel processing and its characterization studies, Mater. Chem. Phys. 189 (2017) 50–55. https://doi.org/10.1016/J.MATCHEMPHYS.2016.12.016.

[37] J. Li, Z. Jin, Y. Zhang, D. Liu, A. Ma, Y. Sun, X. Li, Q. Cai, J. Gui, Ag-induced anatase-rutile TiO2−x heterojunction facilitating the photogenerated carrier separation in visible-light irradiation, J. Alloys Compd. 909 (2022) 164815. https://doi.org/10.1016/j.jallcom.2022.164815.

[38] R. Sinha, P.S. Ghosal, A comprehensive appraisal on status and management of remediation of DBPs by TiO2 based-photocatalysts: Insights of technology, performance and energy efficiency, J. Environ. Manage. 328 (2023) 117011. https://doi.org/10.1016/J.JENVMAN.2022.117011.

[39] T. Luttrell, S. Halpegamage, J. Tao, A. Kramer, E. Sutter, M. Batzill, Why is anatase a better

photocatalyst than rutile? - Model studies on epitaxial TiO2 films, Sci. Rep. 4 (2015) 1–8. https://doi.org/10.1038/srep04043.

[40] M. Zhang, J. Lei, Y. Shi, L. Zhang, Y. Ye, D. Li, C. Mu, Molecular weight effects of PEG on the crystal structure and photocatalytic activities of PEG-capped TiO2 nanoparticles, RSC Adv. 6 (2016) 83366–83372. https://doi.org/10.1039/c6ra12988a.

[41] F. Loosli, P. Le Coustumer, S. Stoll, Impact of alginate concentration on the stability of agglomerates made of TiO2 engineered nanoparticles: Water hardness and pH effects, J. Nanoparticle Res. 17 (2015) 1–9. https://doi.org/10.1007/s11051-015-2863-2.

[42] H. Asadzadeh Patehkhor, M. Fattahi, M. Khosravi-Nikou, Synthesis and characterization of ternary chitosan–TiO2–ZnO over graphene for photocatalytic degradation of tetracycline from pharmaceutical wastewater, Sci. Rep. 11 (2021) 1–17. https://doi.org/10.1038/s41598-021-03492-5.

[43] A. Sharma, N. Liu, Q. Ma, H. Zheng, N. Kawazoe, G. Chen, Y. Yang, PEG assisted P/Ag/Ag2O/Ag3PO4/TiO2 photocatalyst with enhanced elimination of emerging organic pollutants in salinity condition under solar light illumination, Chem. Eng. J. 385 (2020) 123765. https://doi.org/10.1016/j.cej.2019.123765.

[44] S. Wooh, N. Encinas, D. Vollmer, H.J. Butt, Stable Hydrophobic Metal-Oxide Photocatalysts via Grafting Polydimethylsiloxane Brush, Adv. Mater. 29 (2017) 1604637. https://doi.org/10.1002/adma.201604637.

[45] X. Hu, Q. Zhu, X. Wang, N. Kawazoe, Y. Yang, Nonmetal-metal-semiconductor-promoted P/Ag/Ag2O/Ag3PO4/TiO2 photocatalyst with superior photocatalytic activity and stability, J. Mater. Chem. A. 3 (2015) 17858–17865. https://doi.org/10.1039/c5ta05153c.

Figure

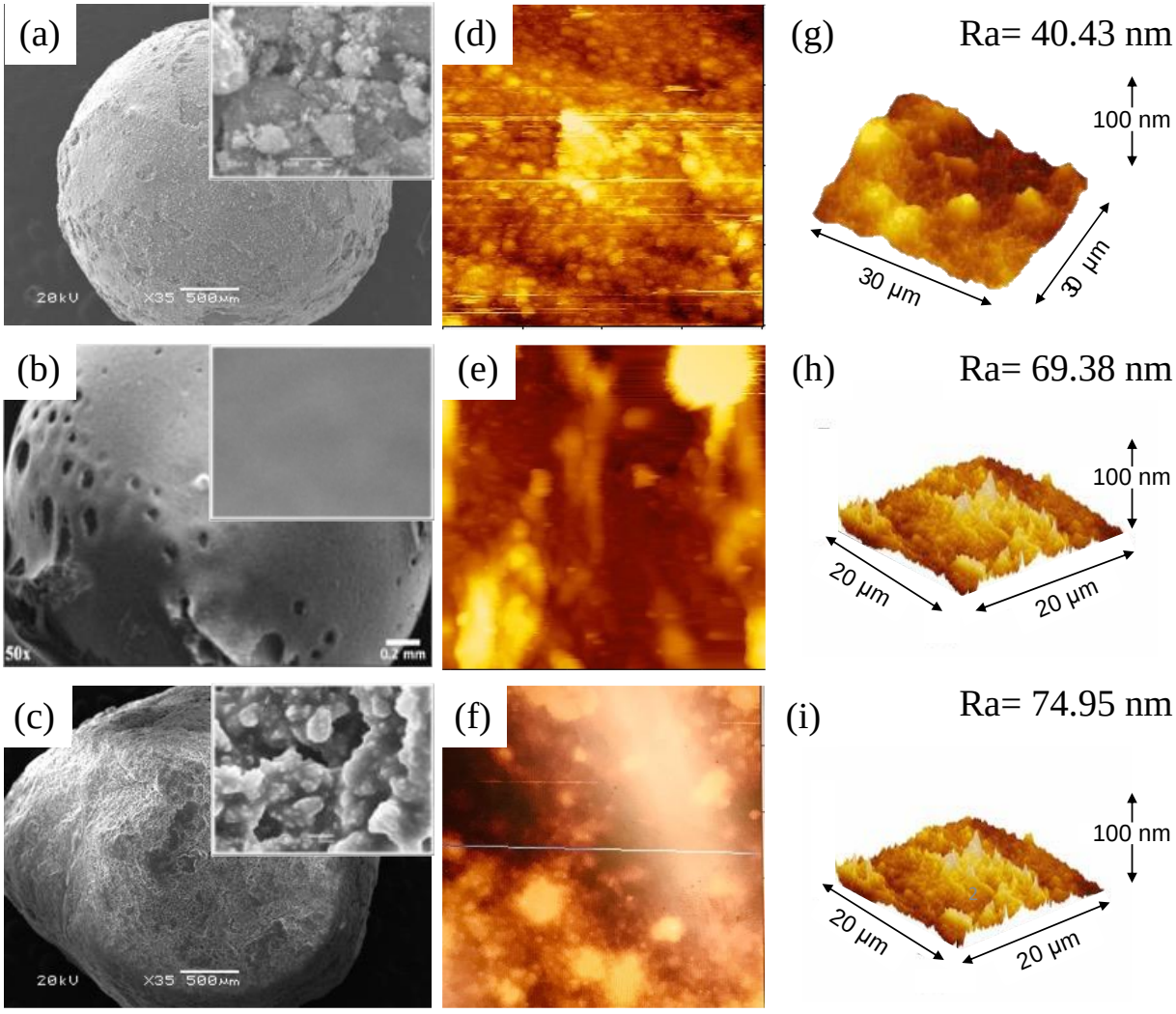

Fig. 1. SEM images of (a) Dip-coated TiO_2, (b) PVA/TiO_2, (c) S-TiO_2 (50 x magnification). Inset images (magnification 3000x). AFM images of (d) Dip-coated TiO_2, (e) PVA/TiO_2, (f) S-TiO_2, and corresponding 3 D images (g) Dip-coated TiO_2, (h) PVA/TiO_2, (i) S-TiO_2.

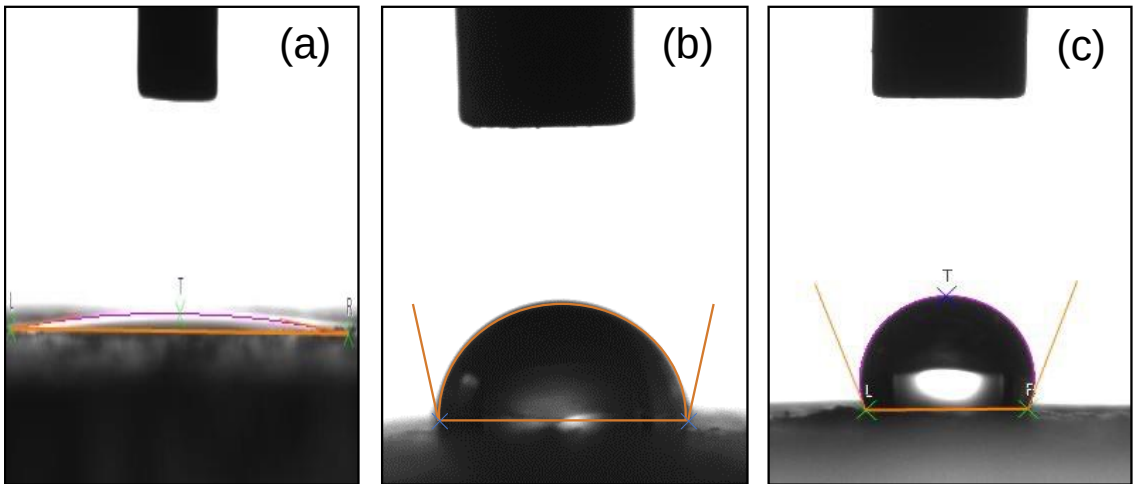

Fig. 2. The water contact angle measurements of immobilized photocatalysts. (a) dip-coated TiO_2, (b) PVA/TiO_2, (c) S-TiO_2. (Volume of water: 10 uL)

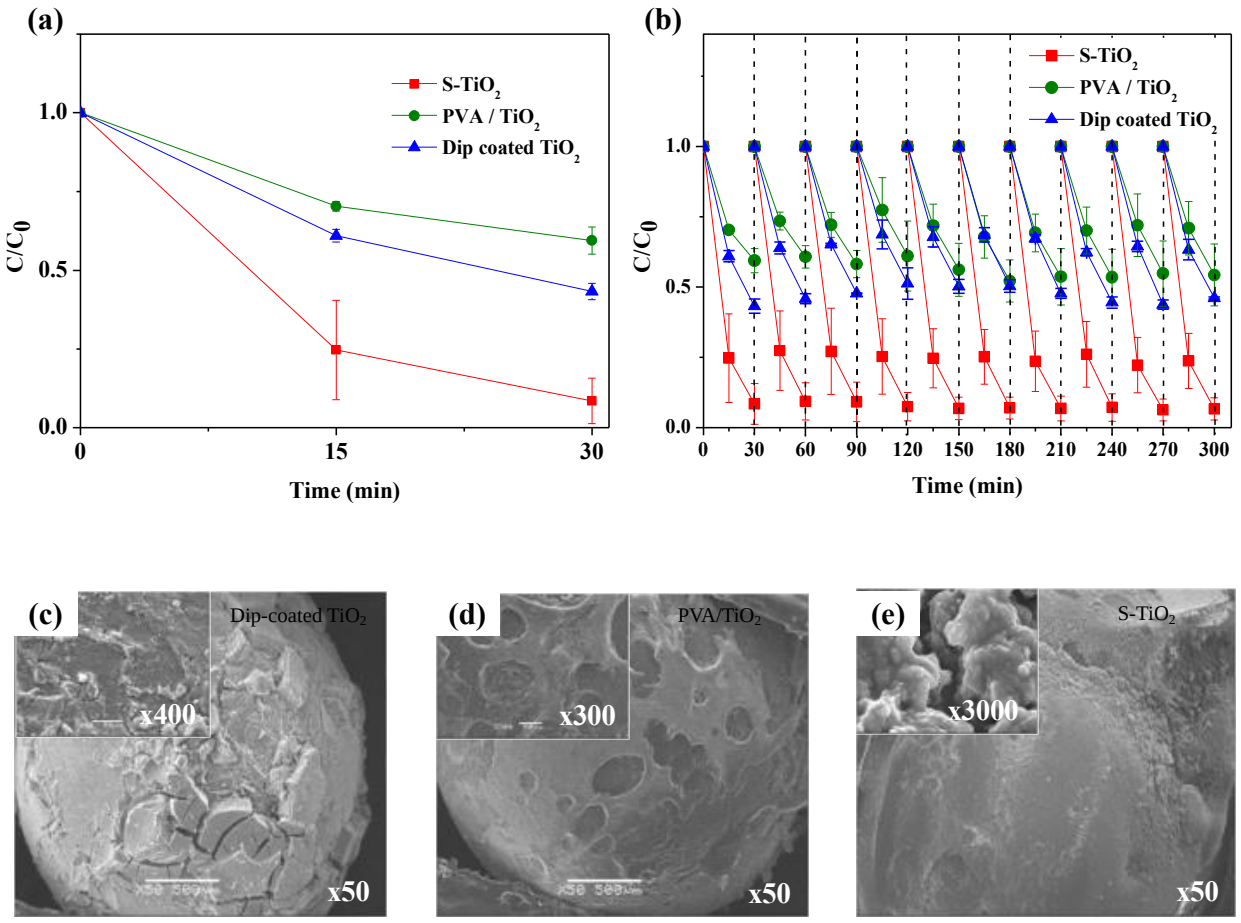

Fig. 3. The comparative study of photocatalytic performance and stability of S-TiO_2, PVA/TiO_2 and dip-coated TiO_2 photocatalyst. (a) photocatalytic reduction of Rh B, (b) recyclability and (c)-(e) scanning electron microscope images of immobilized photocatalysts after 10 repetitive cycles. (Rh B: 2 mg L^{-1}, 50 mL, pH: 7, temperature: ambient, flow rate: 150 mL min^{-1}, light intensity: 550 W m^{-2})

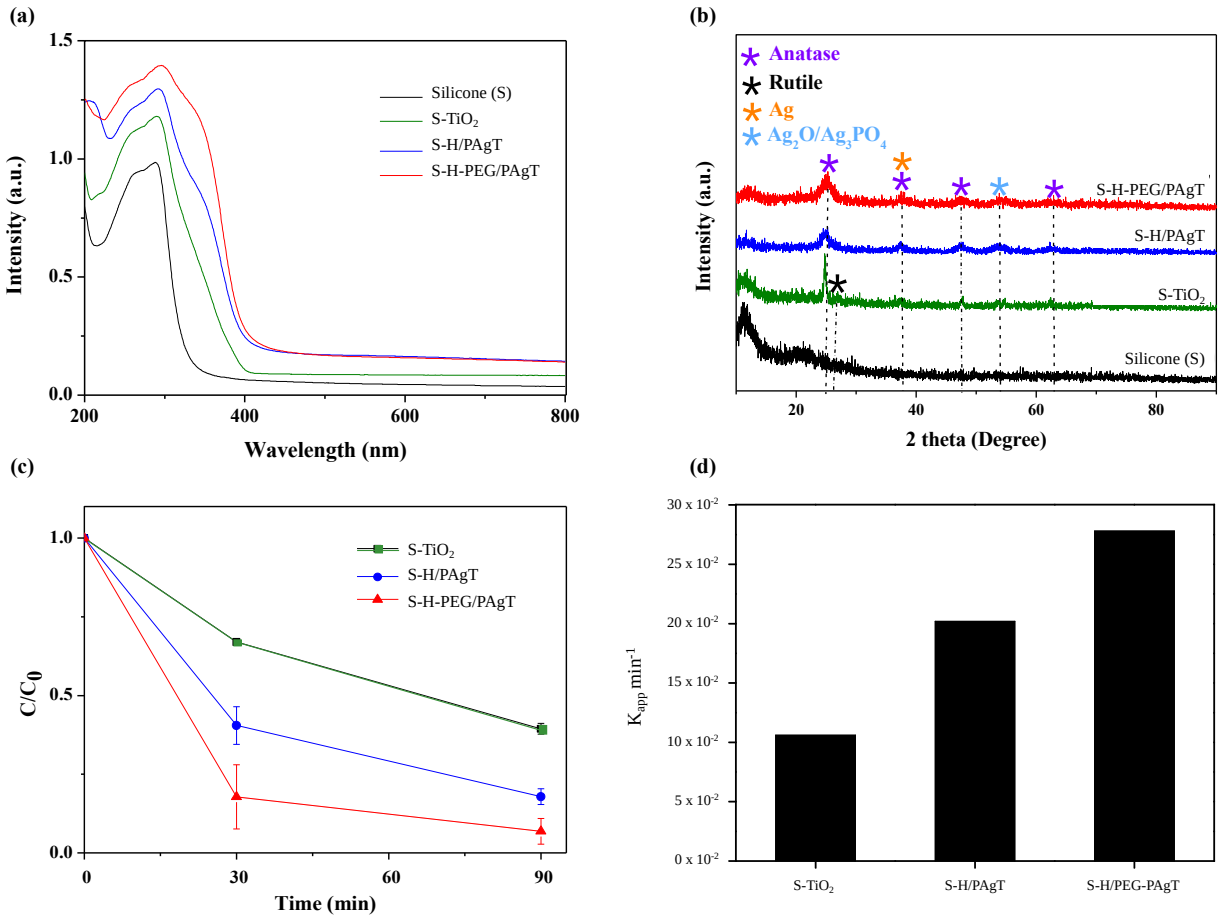

Fig. 4. (a) Diffuse reflectance spectroscopy, (b) x-ray diffraction patterns, (c) TC photocatalytic degradation efficiency, and (d) degradation rate of S-H/PAgT, S-H-PEG/PAgT, and S-TiO_2 (control). Temperature: ambient, flow rate: 150 mL min^{-1}, pH: 7, light intensity: 550 Wm^{-2}, TC: 10 ppm, 50 mL.

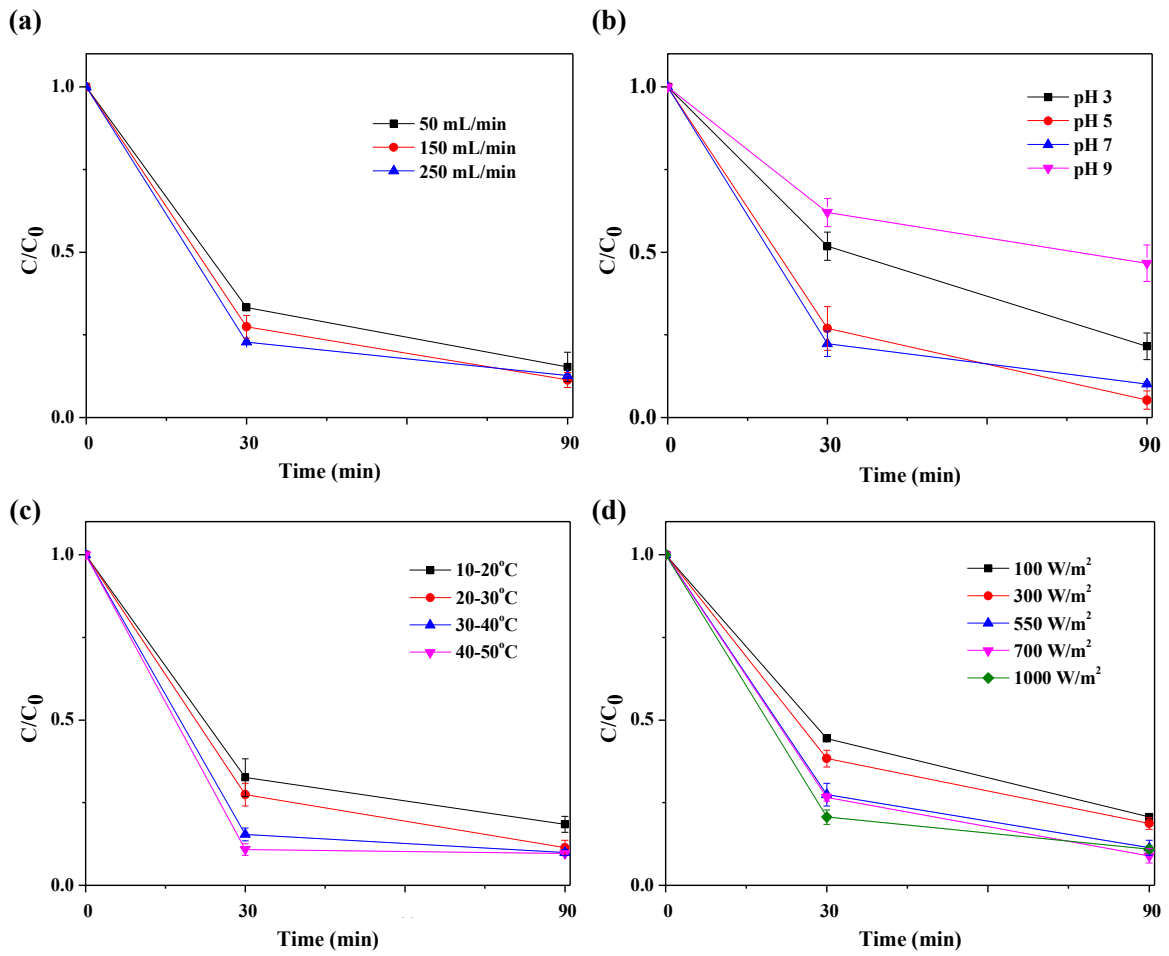

Fig. 5. The S-H-PEG/PAgT photocatalytic degradation of TC under different environmental factors. (a) flow rate, (b) pH, (c) temperature, and (d) light intensity. The reaction conditions of photocatalyst are the same unless mentioned (Temperature: ambient, flow rate: 150 mL min^{-1}, pH: 7, light intensity: 550 Wm^{-2}).

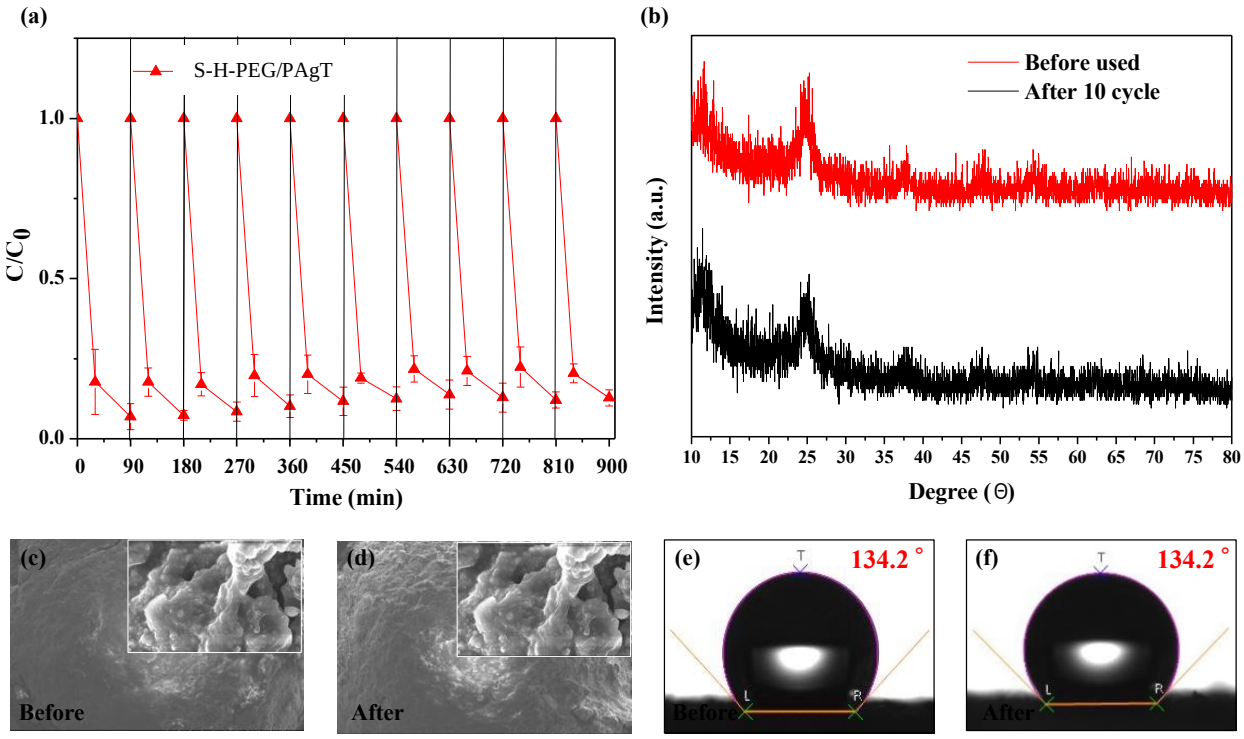

Fig. 6. Repetitive experiments for TC degradation using S-H-PEG/PAgT photocatalyst under solar light irradiation. (a) 10 cycle repetitive, (b) XRD patterns, (c-d) SEM (e-f) water contact angle. Temperature: ambient, flow rate: 150 mL min^{-1}, pH: 7, light intensity: 550 Wm^{-2}.

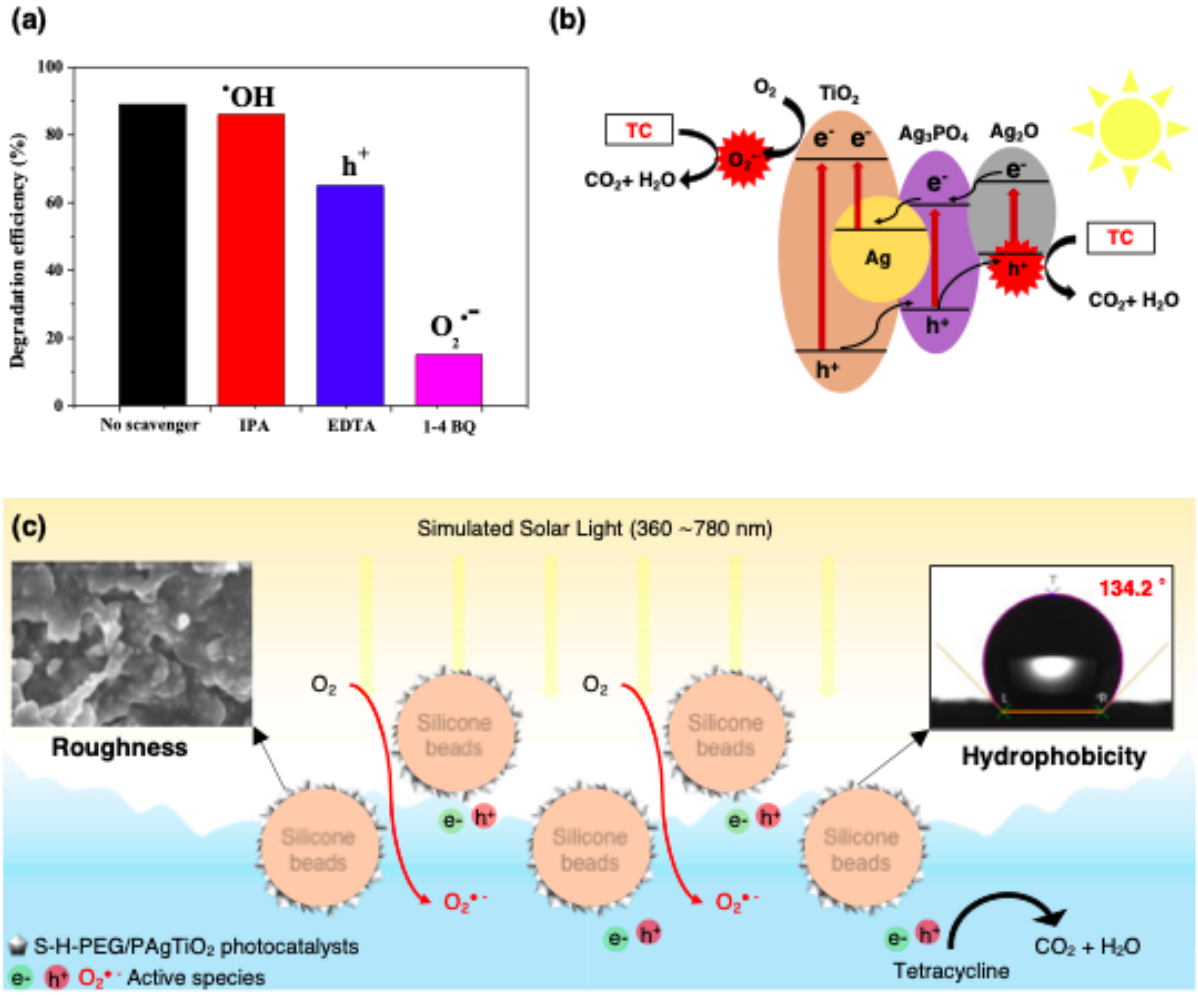

Fig. 7. The proposed mechanism for S-H-PEG/PAgT photocatalytic system for removal of organic pollutants under solar light. (a) The scavenger study, (b) S-H-PEG/PAgT photocatalytic generation of active species and (c) surface characteristics synergistic effect on photocatalysis. Temperature: ambient, flow rate: 150 mL min^{-1}, pH: 7, light intensity: 550 Wm^{-2}, Scavengers concentration: 1M.